

# Development of a Microcontroller System for Optimal Monitoring and Control for Solar Heating

Zhooardbek Zhumakulov<sup>1\*</sup>, Sirojiddin Ergashev<sup>2</sup>, Zaripbek Aidarbekov<sup>1</sup>, Atabek Zhoroiev<sup>1</sup>, Aigul Satibekova<sup>1</sup>, Zarif Umurov<sup>3</sup>

<sup>1</sup>Osh State University, Institute of Mathematics, Physics, Engineering and Information Technology, Department of Power Engineering, Osh, Kyrgyzstan

<sup>2</sup>Fergana Polytechnical Institute, Fergana, Uzbekistan

<sup>3</sup>Bukhara State Pedagogical Institute, Bukhara, Uzbekistan

**Abstract.** A system based on a microcontroller was made to improve the monitoring and control functions of solar heating systems. The proposed model combines multiple sensors and a photodetector into a single-circuit solar system. Its goal is to improve the efficiency of solar collectors in different weather conditions. The main part of this system is an ATmega16 microcontroller, which processes data from the temperature sensor and photodetector. This lets the pump control the flow of coolant in real time. After engineers create the control algorithm, they can use direct solar irradiance measurements to change the speed of the pump so that heat is transferred as efficiently as possible all day long. Smart light management features in the technology help it reach two goals: it changes its responses to changes in sunlight and uses less power by turning off when there is less light. Our experimental data shows that the microcontroller improves the performance of the solar heating system by making it more stable and energy-efficient. This technology implementation has the potential to improve the automation of renewable energy systems, which will lead to long-lasting, efficient solutions.

## 1 Introduction

Solar heating systems are now a common way to turn solar energy into electricity for homes, businesses, and factories [1-3]. These systems are becoming more popular because they are cheap, save energy, and are good for the environment [4-5]. The efficiency of a solar heating system depends a lot on the monitoring and control systems that make sure the system runs safely and uses energy efficiently. According to research in [6], microcontroller-based systems work well together to automate and improve solar heating systems. Microcontrollers changed renewable energy systems by giving them quick access to important information and the ability to make quick decisions [7]. Small, cheap microcontroller systems run advanced optimization algorithms well to make old control

---

\*Corresponding author: [bdosonov@oshsu.kg](mailto:bdosonov@oshsu.kg)

systems work better [8]. Because of advances in technology, modern solar thermal systems need microcontrollers as key parts [9]. Microcontroller systems use sensors and actuators to analyze and manage energy-efficient operation and longer system life through advanced communication methods [10].

Solar heating systems are becoming more and more popular, but they still have problems with heat loss, energy conversion inefficiency, and limited control mechanization [11]. Conventional systems operate within a preprogrammed range that does not account for changing environmental factors such as variations in solar radiation, temperature fluctuations, and shifting demand data [12]. Combining adaptive control systems with dynamic reaction capabilities to achieve optimal system functionality is an immediate operational necessity [13].

The immediate operational requirement is to develop dynamic reaction abilities to maximize system functionality [13]. Real-time adaptation solutions emerge from microcontroller-based systems to handle current operational problems [14]. Microcontrollers achieve continuous monitoring of critical system parameters including flow rate and fluid temperature and solar intensity which enables them to adjust system performance levels automatically [15]. Microcontroller versatility enables both better energy performance concomitantly with reduced operational expenses and fewer operator-involved tasks. The usability of microcontroller systems increases when they integrate Internet of Things (IoT) features to permit real-time monitoring and predictive system maintenance operations.

## 2 Main Part

A solar system functions using an automatic microcontroller control system which enables operation through its structural diagram. A standard single-circuit solar system appears in Figure 1 according to this article. The solar collector exit features Dt1 as a temperature sensor for measurement alongside FR1 as a photoreceiver to measure daytime solar illumination levels. A Dt3 sensor located at the tank top monitors the water temperature that exists in the storage tank. The Dt2 temperature sensor operates at the heat exchanger outlet. A pump (H1), whose speed is regulated by the control microcontroller, is situated between the heat exchanger's outlet and the solar collector. The entire control system operates in accordance with the algorithm described subsequently.

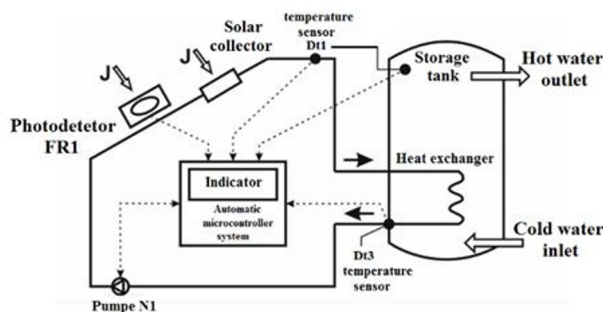


**Fig. 1.** Algorithm for setting up an automatic microcontroller control system.

The tuning algorithm is based on the principle of identifying the point of maximum heat transfer, which corresponds to a specific level of solar activity detected by the photodetector. The process involves gradually increasing the speed of the pump until the temperature sensor at the heat exchanger outlet reaches its maximum value. This temperature corresponds to the inflection point on the curve of the mathematical model.

The solar activity level and pump speed at this optimal point are then automatically recorded in the memory chip.

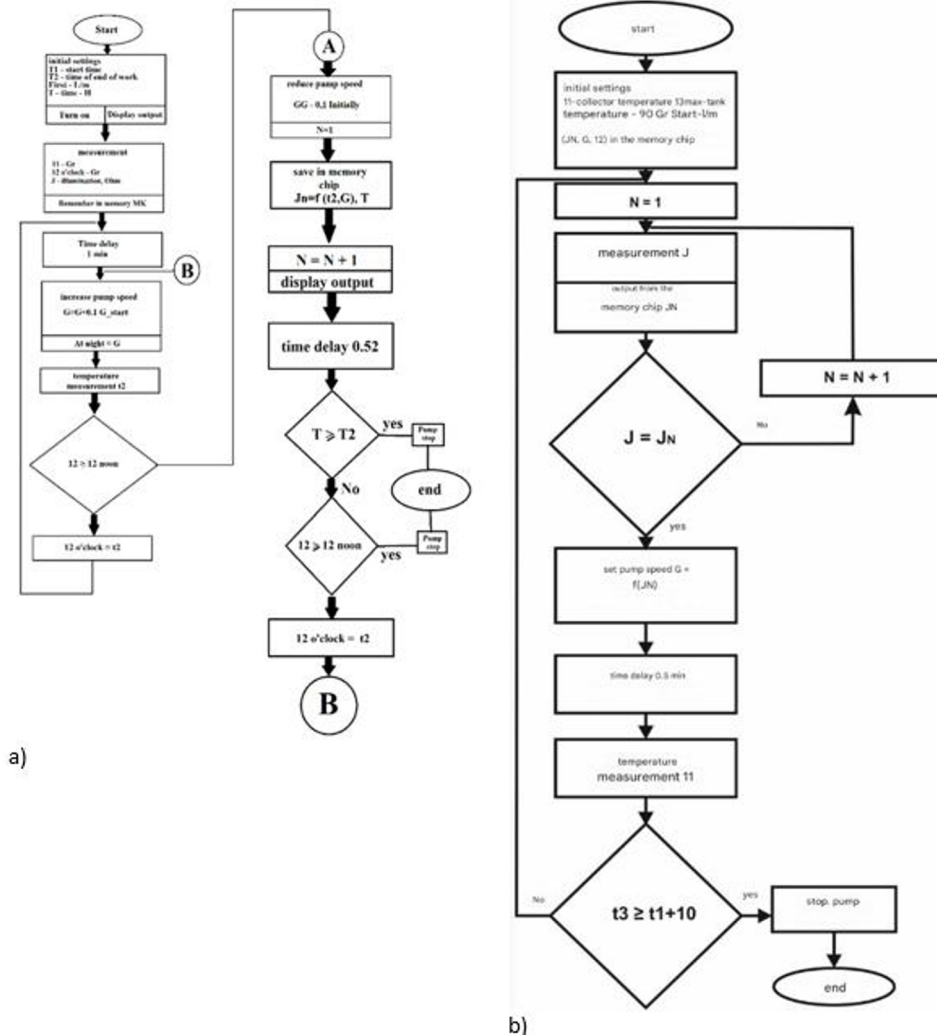


**Fig. 2.** Algorithm of operation of the automatic microcontroller control system (a), benefits of using microcontroller control for optimal operation of solar heating system (b).

The operation of the system relies on comparing the current solar activity level with values previously stored in the memory chip. If the measured value matches any recorded value, the pump is activated at a speed that corresponds to the specific solar activity level established during system setup. This mechanism helps identify shading modes as reductions in solar activity. The pump is turned off once the temperature in the tank reaches its maximum value.

**Key Features and Advantages of Advanced Solar Control Systems:**

1. The ability to automatically adjust the flow rate of the coolant in the solar system (control of the circulation pump flow rate) depends on the temperature difference between the solar collector and the solar system storage tank.

As a result, the solar system operates more stably, the required temperatures are reached faster, additional heat energy is generated by increasing the operating time of the solar

system in the morning, evening hours and in cloudy weather, and energy savings are achieved by the solar system by reducing the power consumption of the circulation pump.

2. Universality of solar controllers. All models of solar controllers can be used in solar systems of various purposes, for example: hot water supply, water heating, heating.

3. High reliability of solar controllers. This is achieved thanks to optimally selected components in solar controllers, enclosed in a sealed polycarbonate case, which provides protection from direct water jets (protection class IP 65). Each solar controller undergoes rigorous testing to identify possible faults at the stage of solar controller development.

4. Easy control of solar system modes. With the help of the indication on the front panel of the solar controller, it is easy to control the state of the solar system. The solar controller does not require constant adjustment; the installation organization carries out all necessary installations of the solar system during the installation process.

5. Remote control of the solar system and adjustment of the solar heating system. Solar controller operation by timer.

6. Memory protection in case of power failure. In case of power failure, the solar controller saves the set parameters of the solar system without changes. When the voltage appears, the solar controller returns to the set operating mode.

Functional diagram of the automatic microcontroller control system:

The entire system is managed by the ATmega16 microcontroller. Real-time signals from the timer chip are relayed to the microcontroller's input. Initial operating modes are established using buttons for initial settings. Control signals are transmitted to the microcontroller from the photoreceiver and sensors Dt1, Dt2, and Dt3. A symmetrical thyristor then supplies voltage to the pump speed control unit. All pertinent information is displayed on a liquid crystal display, and the system is powered by a +5 Volt power supply.

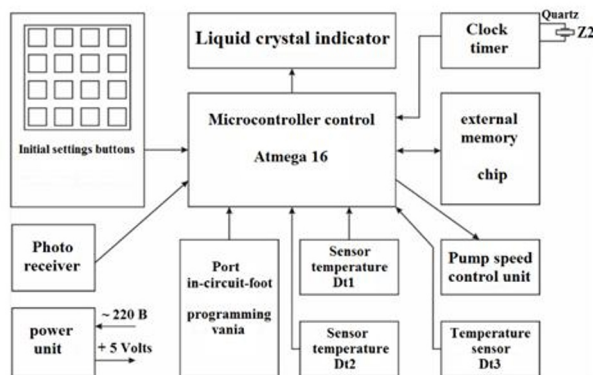


**Fig. 3.** Description of the element base

The ATmega16 microcontroller is an 8-bit high-performance AVR device known for its low power consumption. It incorporates advanced RISC architecture, offering 130 high-performance instructions where most are executed in a single clock cycle. It is equipped with 32 8-bit general-purpose working registers and operates completely statically. The performance of this microcontroller can approach 16 MIPS when operated at a 16 MHz clock frequency and it includes a built-in 2-cycle multiplier.

For memory and storage, the ATmega16 features 16 KB of In-System Self-Programmable Flash memory, which supports up to 1000 erase/write cycles. It also includes 512 bytes of EEPROM and 1 KB of on-chip SRAM, both supporting up to 100,000 erases/write cycles. The hardware supports an alternate boot code sector, and a boot program enables in-system programming, together with Read-While-Write mode access.

The ATmega16 uses IEEE 1149.1 compliant JTAG as its communication interface to support peripheral scanning and provides robust built-in debugging capabilities. A programming solution enabled through the JTAG interface permits modification of Flash memory and EEPROM storage together with jumper controls and lock protections.

Each Timer-Counter type on the microcontroller contains two 8-bit peripherals along with a single 16-bit peripheral which has independent prescale configurations and various operational functionalities such as compare modules and capture modules and PWM features. The device includes an independent oscillator for real-time counting operations along with four PWM channels and eight channels of 10-bit Analog-to-Digital conversion. The device supports eight single-ended and up to seven differential channels through its TQFP package and enables users to program two differential channel gains to specified values from 1 to 10 to 200. This microcontroller supports a byte-oriented 2-wire serial interface in addition to a programmable serial USART and a Serial SPI interface that functions in master and slave modes. The controller incorporates a watchdog timer that functions with integrated oscillator components to provide enhanced safety along with built-in analog comparator capabilities. The microcontroller has special features like power-on reset and short-term supply voltage drop detection that make the system more reliable. The built-in calibrated RC oscillator and different ways to interrupt the system make it more reliable. The MCU has six power-saving modes that let it manage power intelligently in a variety of situations, such as Idle, Power-save, Power-down, Standby, Extended Standby, and ADC noise reduction.

The physical layout information, which includes accurate ATmega16 pinout diagrams, gives developers more options for how to use the ATmega16 in different electronic projects.

The DS18B20 digital thermometer has a single-wire 1-Wire interface and adjustable conversion bits, so it can be used in a variety of situations with high accuracy. The device makes digital codes directly from measurements between  $-55^{\circ}\text{C}$  and  $+125^{\circ}\text{C}$ , so there is no need to convert them before they can be used. The built-in ADC resolution can be set between 9 and 12 output code bits, depending on how precise the application needs to be.

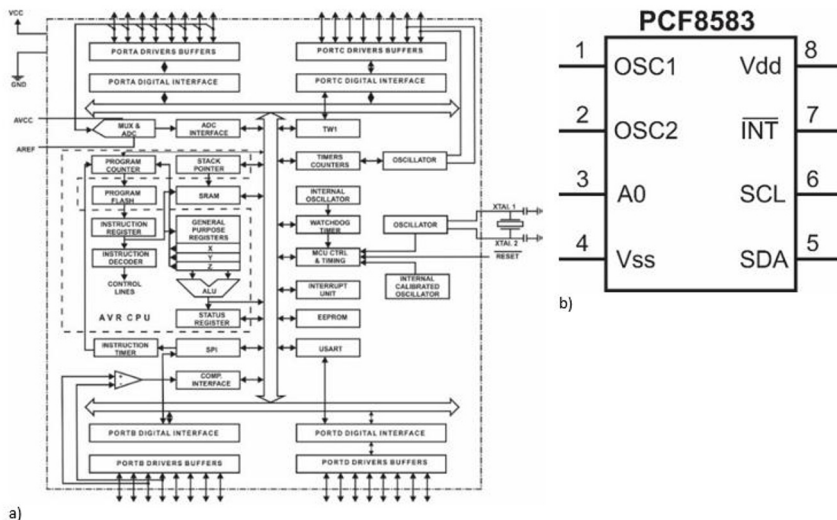


**Fig. 4.** Description of temperature sensor DS18B20 (a) and PCF8583 Real Time Clock IC (b).

The thermometer does absolute conversions with errors of less than  $0.5^{\circ}\text{C}$  in the controlled temperature range of  $-10^{\circ}\text{C}$  to  $+85^{\circ}\text{C}$ . It also does full 12-bit conversions in 750 milliseconds. The device has non-volatile memory that can store adjustable temperature thresholds, and it guarantees reliable performance through customizable settings. The

DS18B20 has built-in logic that sends priority signals through the 1-Wire line when the temperature goes above a certain level, which makes it more reliable in important situations.

The device's 1-Wire interface is designed to theoretically allow an unlimited number of similar devices to be addressed on a single 1-Wire line. This is especially useful for complex systems that need a lot of sensors. Each thermometer has its own 64-bit registration number (group code 028H) that helps keep the system organized and easy to keep an eye on. The 1-Wire line gives this thermometer parasitic power, so it doesn't need an outside power source. This makes both installation and maintenance easier. The DS18B20 is offered with three packaging options available: TO-92 transistor package, 8-pin SO package (DS18B20Z) for surface mounting and 8-pin micro-SOP package (DS18B20U) for surface mounting.

The DS18B20-PAR exists as a modified version built exclusively to function from parasitic power supply sources. The TO-92 package of this version employs two terminals out of three for maximum power efficiency. Multiple available packaging designs and special versions of the DS18B20 make these sensors adaptable to different temperature applications in diverse industrial settings.

A standard integrated circuit with EEPROM functionality includes specified pin assignments in a particular configuration. The external generator connects its frequency (32768Hz) through OSC1 while delivering its output at OSC2. The JSC line operates as a selection system to deliver varying device addresses. NELAND- which stands for common ground or power supply wire- is labeled Vss and the main power supply line operates under the Vdd designation. Synchronized communication through I2C bus occurs via the SDA data line while also using the SCL clock signal line to carry data. Proper functioning of the external devices requires a pull-up resistor to operate the INT pin which generates interrupts.

As part of its fabrication ATMELCORP produced the electrically erasable (EEPROM) memory chip model AT24C64N-10SI-2.7 designed for demanding high-performance applications. Users can store extensive data through the 8Kx8 bit memory organization provided by EEPROM. Data access requires only 100 nanoseconds because of its fast performance speed. The proven durability of the EEPROM results from its capacity to perform 1,000,000 recording cycles without failing thus ensuring reliable operation during extended use periods. Serial device communication runs through a serial interface that brings together smooth connections and rapid data-sharing capabilities. This storage device functions between 2.7 volts and 5.5 volts power supply and maintains adaptability across different power networks. The system operates efficiently while consuming limited power through its operating current rates of 3 mA and its standby current rates of 2 uA. Temperature fluctuations between 40°C and +85°C allow this device to efficiently perform in multiple environmental conditions throughout its wide range of applications.

### **3 Development of a basic microcontroller control scheme**

Microcontroller circuit design calculation: The AVR series microcontroller implements multiple integrated timers in its design. Embedded systems require essential timers to perform different timing operations. A set of timers exist in two fundamental types distinct types: general-purpose timers and watchdog timers. General-purpose timers feature widespread applications throughout different systems. Watchdog timers exist to automatically reset the microcontroller by design but general-purpose timers serve diverse system functions non-responsive or "freezes." Among the timers inside an AVR microcontroller each one uses its own count register. Eight-bit timers utilize an eight bit The county register operates through a sixteen-bit count register but eight-bit timers function with an eight-bit count register. These storage elements possess critical importance

since they retain running timer values. Digital timers maintain their present counting numbers to perform both I/O computations. For instance, the count register for an eight-bit The registers that store timer counts employ naming patterns where "x" stands for either the TO timer TCNT0 or the T2 timer TCNT2. Similarly, the storage of most significant timer values with sixteen-bit timers depends on two separate registers named 'H' which appear at the final segment of the register label. The Time Constant 'r' depends on the product of the capacitor C10 with the resistor R19. The registers divide into a most significant part (marked 'H') and a least significant part which displays an 'L'.

These count registers, such as TCNT1H and TCNT1L for timer T1, and TCNT3H and TCNT3L for timer T3, are designed to handle data efficiently. The microcontroller can modify or read the value of any count register at any given time. When a timer is activated in counting mode, it starts receiving counting pulses at its input. These pulses add one to the count register every time they are received, whether they come from the microcontroller's internal clock or from specific pins on the microcontroller.

When the count register is full, it overflows, goes back to zero, and starts counting again. This overflow event can cause interrupts, which are an important part of the microcontroller's interrupt system. Timers can cause interrupts in a number of ways, such as when they overflow or when a specific function, like a watchdog timer, is called. This shows how important and flexible timers are in microcontroller applications. These features make AVR timers great for controlling precise time-based tasks in embedded systems, making sure they are both flexible and reliable. Figure 5 (a) presents the diagram of the control microcontroller.

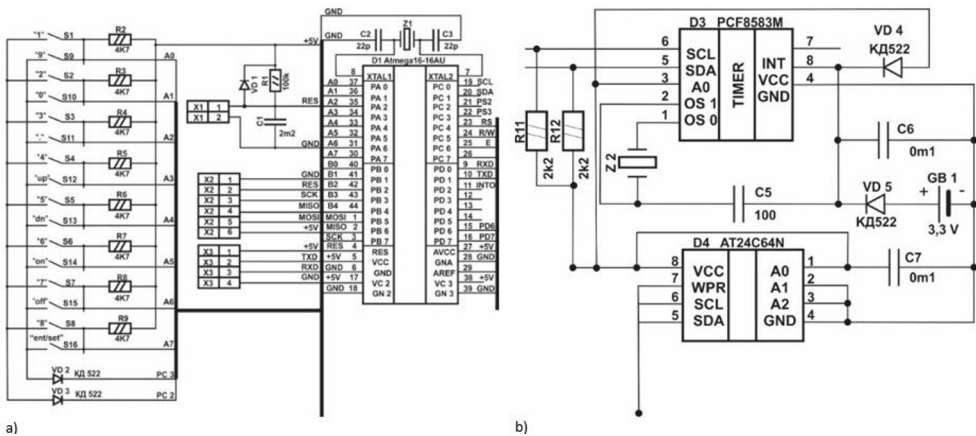


**Fig. 5.** Schematic Diagram of the Control Microcontroller (a) and Circuit Diagram for Real-Time Mark Setting in the Microcontroller (b).

The control microcontroller is clocked by the frequency of the quartz resonator Z1 and stabilized by capacitors C<sub>2</sub>, C<sub>3</sub> - 22 picofarads. The following are connected via the microcontroller bus: X<sub>2</sub> - in-circuit programming port; X<sub>3</sub> - RS serial port for communication with other devices.

The VD1, R1, C1 circuit serves to generate voltage at the RES input of the microcontroller, which supports the storage of the recorded program. The program is reset via the X1 connector. The current at the RES input is:

$$I_{RES} = UPIT/R_1 = 5B/100K = 50\mu A \tag{1}$$

The initial settings are programmed using the SI - S16 buttons via the limiting resistors  $R_2 - R_9$ . The nominal input current at the microcontroller inputs is 1.1 mA. Let's calculate the resistance of the resistors  $R_2 - R_9$ :

$$R_2 = U_{pit}/I_{in} = 5V/1.1mA = 4.7 k\Omega \quad (2)$$

Diodes VD2, VD3 serve to divide 16 buttons into “two by eight”.

Calculation of the timer circuit with a memory chip:

For stable operation of the microcontroller, the D3 chip is included in the circuit, which sets real time marks. (Figure 8). Time setting chain - Z2, C5. For the timer to operate in autonomous mode, the battery GB1 is included.

All data on solar illumination and temperatures are stored in the D4 memory chip, since storing data in the microcontroller memory is not always reliable. Capacitors C6 and C7 filter interference in the power supply circuit. The current at the SCL, SDA inputs of the D3, D4 chips is 2.3 mA. Let's calculate the resistance of resistors R11 - R12:

$$R_{12} = U_{pit}/I_{inDCL} = 5V/2.3mA = 2.2 k\Omega \quad (3)$$

Calculation of the LCD circuit: Variable resistor R10 (Figure 8. (a)) adjusts the contrast of the indicator. The resistance of resistor R10 is calculated using the formula:

$$R_{10} = 0.5 \cdot U_{power}/I_{V0} = 2.5 V/0.16 mA = 15 k\Omega \quad (4)$$

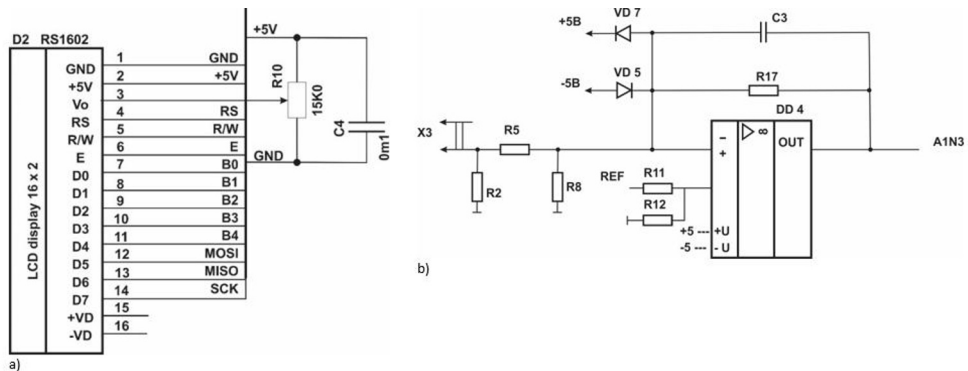


**Fig. 6.** Diagram of Variable Resistor R10 for Contrast Adjustment (a) and Schematic Diagram of the Photodetector Circuit (b).

Capacitor C4- for power supply +5 Volts, filters high-frequency interference. This block gets an analog signal from a photodetector that is between +5 and 0 volts and sends it to the controller for more processing. Figure 10 shows the photodetector circuit and explains how different parts work together to process and amplify the light signals they get. This circuit employs an integrating amplifier that transforms these light signals into usable electrical output, which can then be accurately measured and analyzed by the system's microcontroller for optimal performance adjustments.

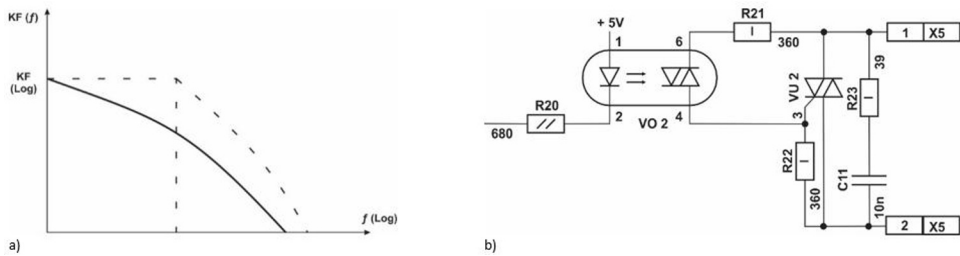


**Fig. 7.** Amplitude-Frequency Characteristic of the Integrating Amplifier (a) and Pump Speed Control Circuit Diagram (b).

This block is based on an integrating amplifier and outputs the sum of linear values  $U_1(t)$ , which are related to very small-time values that happen one after the other. The integrating amplifier raises the level of the signal while changing its shape, without significantly lowering the signal-to-noise ratio. Most importantly, it can multiply the signal by  $K$  times.

The time constant of the integrating amplifier is an important factor that affects how the circuit responds. To find the amplifier's response time, divide  $C_{10}$  by  $R_{19}$ . In this

The timer values have a capacitance of 1 nano farad and a resistance of 100 kilohms. The time constant finds  $\tau$  by using the math that connects the  $C_{10}$  and  $R_{19}$  values in 0.0001 seconds, or  $10^{-4}$  seconds. The defined value controls how quickly the amplifier reacts to changes that come in.

The circuit uses this parameter to manage the input signal properly, which keeps the signal processing working well. This time constant lets you change the amplifier gain so that the inputs and outputs stay in the right matching conditions. The signals operate optimally because input and output impedances correspond for efficient signal processing.

The integrating amplifier's frequency response, shown in Figure 11, also looks like a broken curve with a certain breakup frequency. This characteristic determines how the amplifier will respond over a range of frequencies, ensuring that it meets the necessary specifications for integration and signal processing in the circuit.

In the circuit described, diodes  $VD_7$  and  $VD_6$  act as diode clamps, establishing a voltage corridor for the input signal in the range of  $-5$  to  $+5$  volts. These diodes, in particular models 1N4148 and KD522B, are rated for a maximum reverse voltage of 50 V and a peak current of 100 mA. This setting ensures that the input voltage remains within safe operating limits, preventing potential damage to other components in the circuit.

## 4 Description of the operation of the basic diagram of the automatic control system

The basic diagram is shown in Figure 1.20. The PA microcontroller port serves the buttons for setting the initial settings. The RV port is connected to the X2 in-circuit programming connector for entering the working program according to the algorithm. The RV port is also connected to the X3 connector - the COM port for communication with computers in the case of a remote control and monitoring of the system. The same port is connected to the liquid crystal indicator, which displays the current information.

The D3 timer-counter with a built-in real-time clock is connected to the PC port. The timer microcircuit sets the exact time by which current information is written into the memory. The timer circuit includes a galvanic element for constant counting in the event of a power failure. The timer operation is stabilized by a Z2 quartz resonator.

The external D4 memory chip is designed to store data on time, solar illumination and temperatures. Its use in this circuit makes the system more stable and enables recording in the amount of 64 kilobytes. This chip is also connected to the PC port of the microcontroller.

All input and output peripherals are connected to the PD port of the MC. To measure temperatures from various points of the solar system, the circuit includes high-precision digital temperature sensors DD6, DD7, DD8 of the DS18B20 brand. A signal processing unit from the photodetector is built based on the DD9 microcircuit. A standard photoresistor is used as a photodetector, which converts solar radiation energy into electric current energy. The measured current is amplified by the microcircuit and fed to the microcontroller input.

The pump speed control circuit is based on the VU2 simistor, which is fully compatible with the electric pump in terms of power parameters. Optocoupler V02 is used for galvanic isolation of the power section and the microcontroller. The electric pump speed is changed by controlling the pulse-width modulation generated at the microcontroller output. The entire control system circuit is powered by a power supply that generates a voltage of +5 Volts. The circuit elements are located on a board based on double-sided textolite.

## 5 Conclusion

The thorough examination of the solar heating system uncovered a multifaceted correlation between heat transfer rates and numerous variables. A thorough investigation revealed that merely a fraction of these attributes could be incorporated into the mathematical model formulated for control optimization. This model helped create a computational framework for optimal control that takes into account how solar activity changes over time. This is important because it has a big effect on how the microcontroller-based control system works.

The influence of seasonal and daily variations in solar activity is important, directly influencing the control system's adjustment of the electric pump speeds to change the flow characteristics. This knowledge led to the development of advanced algorithms that make it possible to set up and keep an eye on the solar heating system. The setup process is meant to find the right pump speeds for different levels of solar activity and save this information in the system's memory so it can be easily accessed and used.

The operational algorithm also turns on the pump at speeds that are proportional to the recorded solar irradiation values. This makes sure that the system can easily adapt to changes in the weather. The way the functional and basic diagrams of the control system are set up shows how strategic planning is used to make the system work better overall.

The integration of parts like the mP7805 and K142EN5V voltage stabilizers also makes sure that the solar system works well by giving it a reliable power source that keeps the microcontroller's performance stable even when the power supply changes. These stabilizers not only keep the voltage steady, but they also make the system more reliable and stronger, which keeps the solar heating control system running at the same level of efficiency. An automated microcontroller control system with carefully designed algorithms and reliable power supply parts makes the system much more efficient and reliable. This method makes the control process better and the solar heating system work better overall. It shows how integrated control systems can be useful in renewable energy applications.

## References

1. Qusay Hassan et al. A review of hybrid renewable energy systems: Solar and wind-powered solutions: Challenges, opportunities, and policy implications. *Results in Engineering* 20 (2023) 101621. <https://doi.org/10.1016/j.rineng.2023.101621>.
2. Akhmadov, K.S., Akhatov, J.S. & Xin, L. Geometric Optimization of a CeO<sub>2</sub>-Based Solar Thermochemical Reactor for Hydrogen Production: Temperature Distribution Analysis under 2 kW Concentrated Solar Power. *Appl. Sol. Energy* 61, 102–115 (2025). <https://doi.org/10.3103/S0003701X25600729>.
3. Pérez, R.; Fernández, C.; Laca, A.; Laca, A. Evaluation of Environmental Impacts in Legume Crops: A Case Study of PGI White Bean Production in Southern Europe. *Sustainability* 2024, 16, 8024. <https://doi.org/10.3390/su16188024>
4. Askarov M.N, Juraev A.R, Nazarova S.M, Ahmadov Kh.S. Thermal Effects of Water-Absorbing Porous Materials. Sixteen International Conference on Thermal Engineering: Theory and Applications. June 18-20, 2025 Bucharest, Romania. <https://journals.library.torontomu.ca/index.php/ictea/article/view/2525>.
5. T. Falope et al. Hybrid energy system integration and management for solar energy: A review. *Energy Conversion and Management: X21* (2024) 100527. <https://doi.org/10.1016/j.ecmx.2024.100527>
6. Ghosh, A. Recent Advances in Renewable Energy and Clean Energy. *Energies* 2022, 15, 3204. <https://doi.org/10.3390/en15093204>.
7. Inna Sosunova et al. IoT-Enabled Smart Waste Management Systems for Smart Cities: A Systematic Review. *IEEE Access*. Volume 10, 2022. DOI:10.1109/ACCESS.2022.3188308.
8. Midriem Mirdanies. Dual-axis Solar Tracking System. A Combined Astronomical Estimation and Visual Feedback. 2016 International Conference on Sustainable Energy Engineering and Application (ICSEEA).
9. Nathan C. Brown et al. The effect of performance feedback and optimization on the conceptual design process. Proceedings of the IASS Annual Symposium 2016 “Spatial Structures in the 21st Century” 26–30 September, 2016, Tokyo, Japan.
10. Dongyang C, Jiewen Z and Xiaolong H (2024) Dynamic adaptation in power transmission: integrating robust optimization with online learning for renewable uncertainties. *Front. Energy Res.* 12:1483170. doi: 10.3389/fenrg.2024.1483170.
11. Kumar L., Ahmed J., El Haj Assad M., Hasanuzzaman M. Prospects and Challenges of Solar Thermal for Process Heating: A Comprehensive Review. *Energies* 2022, 15, 8501. <https://doi.org/10.3390/en15228501>.
12. Deepak Singh et al. Adaptive control strategies for effective integration of solar power into smart grids using reinforcement learning. *Energy Storage and Saving* 3 (2024) 327–340. <https://doi.org/10.1016/j.enss.2024.08.002>.
13. Vinay Pratap Verma. Advancement in Solar Technology: Evolution, Generation, Future Prospective, and Challenges - A Review. DOI:10.20944/preprints202407.0003.v1.
14. Nur Iksan et al. Real-Time Monitoring of Photovoltaic Systems and Control of Electricity Supply for Smart Micro Grid-PV using IoT. *TEM Journal*. Volume 13, Issue 1, pages 514-523, ISSN 2217-8309, DOI: 10.18421/TEM131-53, February 2024.
15. Ozkan, M. Atmospheric alchemy: The energy and cost dynamics of direct air carbon capture. *MRS Energy & Sustainability* (2024). <https://doi.org/10.1557/s43581-024-00091-5>.